Anti-photoaging and anti-oxidative activities of natural killer cell conditioned medium following UV-B irradiation of human dermal fibroblasts and a reconstructed skin model

SUNG-EUN LEE[1,2*], TAE-RIN KWON[1*], JONG HWAN KIM[1,2], BYUNG-CHUL LEE[1,2], CHANG TAEK OH[3], MINJU IM[3], YU KYEONG HWANG[4], SANG HOON PAIK[4], SEUNGRYEL HAN[4], JEOM-YONG KIM[3] and BEOM JOON KIM[1,2]

[1]Department of Dermatology, College of Medicine, Chung-Ang University; [2]Department of Medicine, Graduate School, Chung-Ang University, Seoul 06974; [3]Research Institute, Green Cross WellBeing Corporation, Seongnam, Gyeonggi-do 13595; [4]Cell Therapy Research Center, GC LabCell, Yongin, Gyeonggi-do 16924, Republic of Korea

Received April 10, 2019; Accepted July 19, 2019

DOI: 10.3892/ijmm.2019.4320

Abstract. Conditioned media from various sources comprise numerous growth factors and cytokines and are known to promote the regeneration of damaged tissues. Among these, natural killer cell conditioned medium (NK-CdM) has been shown to stimulate collagen synthesis and the migration of fibroblasts during the wound healing process. With a long-term aim of developing a treatment for skin photoaging, the ability of NK-CdM to prevent ultraviolet-B (UV-B) damage was assessed in neonatal human dermal fibroblasts (NHDFs) and an *in vitro* reconstructed skin model. The factors present in NK-CdM were profiled using an antibody array analysis. Protein and mRNA levels in UV-B exposed NHDFs treated with NK-CdM were measured by western blotting and quantitative reverse transcription-PCR, respectively. The total antioxidant capacity of NK-CdM was determined to assess its ability to suppress reactive oxygen species. The anti-photoaging effect of NK-CdM was also assessed in a 3D reconstituted human full skin model. NK-CdM induced proliferation of UV-B-treated NHDFs, increased procollagen expression, and decreased matrix metalloproteinase (MMP)-1 expression. NK-CdM also exhibited a potent anti-oxidant activity as measured by the total antioxidant capacity. NK-CdM inhibited UV-B-induced collagen degradation by inactivating MAPK signaling. NK-CdM also elicited potential anti-wrinkle effects by inhibiting the UV-B-induced increase in MMP-1 expression levels in a 3D reconstituted human full skin model. Taken together, the suppression of both UV-B-induced MMP-1 expression and JNK activation by NK-CdM suggests NK-CdM as a possible candidate anti-skin aging agent.

Correspondence to: Dr Beom Joon Kim, Department of Dermatology, College of Medicine, Chung-Ang University, 224-1 Heukseok-dong, Dongjak-ku, Seoul 06974, Republic of Korea
E-mail: beomjoon@unitel.co.kr

*Contributed equally

Key words: natural killer cell, conditioned medium, ultraviolet, photoaging

Introduction

Aging is characterized by a gradual loss of the body's structural integrity and physiological functions. Unlike other organs, the human skin is subjected to both intrinsic and extrinsic aging processes (1). Extrinsic aging can be caused by ultraviolet (UV) radiation, stress, or smoking and is characterized by wrinkles, slackness, dryness, and a rough skin tone. Exposure to UV radiation (UV-A, UV-B, and UV-C) is a major cause of skin aging (2). UV-B penetrates the epidermis and the upper part of the dermis, damaging keratinocytes in particular and causing sunburn, photoaging, and skin cancer (3). Exposure of the skin to UV-B radiation increases the production of inflammatory cytokines and matrix metalloproteinases (MMPs) in keratinocytes through the action of activator protein-1 (AP-1) and nuclear factor-κB (NF-κB) (4). The inflammatory cytokines produced in response to UV-B irradiation stimulate fibroblasts to increase the production of MMPs that degrade the extracellular matrix (ECM) (5).

UV-B radiation also promotes the production of reactive oxygen species (ROS) in cells. ROS induce a number of deleterious effects, such as DNA damage, inflammatory responses, and damage to the integrity of the ECM (6). ROS production therefore also plays an important role in skin aging. UV-B-induced ROS production regulates signaling through growth factor and cytokine receptors, many of which lead to the activation of MAPK pathways namely the c-Jun N terminal kinase (JNK), extracellular signal-regulated kinase (ERK), and p38 kinase pathways (7). AP-1, a heterodimer composed of c-Jun and c-Fos, is regulated by c-Jun phosphorylation through the JNK pathway as well as through the expression levels of c-Fos. The resulting increased AP-1 activity increases the production of MMP-1, leading to a decrease in type I procollagen levels and resulting in the breakdown of the ECM of the dermis, which leads to skin aging (8).

The field of cosmetics has been trying to prevent skin aging by studying the mechanisms that regulate the production of type I collagen and/or regulate MMP-1 expression levels. Cosmeceuticals, a compound word for 'cosmetics' and 'medicines' that are able to medically improve the skin's condition, are gaining more and more attention in the cosmetics industry (9). Using medically proven ingredients such as antioxidants [e.g. vitamin C and E (10-12), coenzyme Q10 (13), and phenolic acid derivatives (14)] cosmetics can delay the skin aging caused by physiological environmental factors such as exposure to UV radiation. More recently, the use of human-derived stem cell cultures to regenerate the skin has been proposed (15). The concept is that stem cells can be induced to differentiate into skin cells that can then be used to treat patients with skin damage or to improve the damage caused by skin aging (16). Other approaches including the use of growth factors, natural products, and biologically active peptides have been proposed as treatments to prevent and/or reverse the effects of skin aging (17).

Natural killer cells (NK cells) account for 10-15% of human peripheral blood lymphocytes (18). NK cells are functionally defined by their ability to destroy target cells without restriction by major histocompatibility antigens. The cytokines secreted by NK cells mediate the eradication of pathogens and infected cells and regulate the adaptation of the immune response, providing a means for the dynamic interaction between innate immunity and adaptive immunity (19). The cytokines secreted by NK cells include IL-1β, IL-6, IL-10, IL-12, TNF-α, interferon (IFN)-γ inducible factor, also referred to as transforming growth factor β (TGF-β), IL-15, and IL-18. NK cells can also produce cytokines with antiviral functions such as IFN-γ and TNF (20).

In this study, the anti-wrinkle effects of natural killer cell conditioned medium (NK-CdM) on elastin synthesis, collagen synthesis, and the abundance of MMP-1 and TIMP-1 transcripts and proteins were evaluated using neonatal human dermal fibroblasts (NHDFs). The present study demonstrated that NK-CdM may be a possible candidate anti-skin aging agent.

Materials and methods

Ethics statement. All study samples were obtained after the acquisition of written informed consent from the study participants, in accordance with the Declaration of Helsinki. The research protocol was reviewed and approved by the Institutional Review Board of Seoul National University Hospital (permit no. H-1811-023-985).

NK cell enrichment and expansion. Peripheral blood mononuclear cells were collected from healthy donors (n=3; 2 males and 1 female; average age, 36.6) via lymphapheresis for 2-4 batch productions in February 2019 from Seoul National University Hospital (Seoul, Korea). NK cells present in the mononuclear cells were enriched and expanded with Cellgro SCGM medium (CellGenix) containing human plasma and interleukin-2 for approximately three weeks as previously described (21,22). When the NK cell cultivation was completed, the NK-CdM was harvested by centrifugation at 400 x g for 3 min at 4˚C to remove the NK cells. NK cell concentration at the end of the cultivation process was ~$0.5x10^6$-$2.0x10^6$ cells/ml. The NK-CdM collection and production were performed at GC LabCell.

Neonatal human dermal fibroblast culture. The neonatal human dermal fibroblast cell line (NHDF; C0045C) was purchased from Thermo Fischer Scientific, Inc. The cells were grown in a humidified incubator at 37˚C with a 5% CO_2 atmosphere in Medium 106 (Thermo Fisher Scientific, Inc.) supplemented with 10% (v/v) fetal bovine serum (Gibco; Thermo Fisher Scientific, Inc.) and 0.5% (v/v) penicillin-streptomycin and used up to passage seven. When they were 80% confluent, the cells were sub-cultured by trypsinization. The culture medium was replenished every 48 h.

CCK-8 assay. NHDFs were plated at a density of $5x10^3$ cells/well in 96-well plates, and their proliferation was measured using a Cell Counting Kit-8 (CCK)-8 assay (Dojindo Molecular Technologies, Inc.). Cells were treated, serum-starved for 24 h, and then treated with various concentrations of NK-CdM (2.5, 5, and 10%) for 24 and 72 h. CCK-8 solution (10 µl) was added to the cells in 1 ml DMEM (Thermo Fisher Scientific, Inc.), and incubated for 2 h at 37˚C. Absorbance was measured at 450 nm using a microplate reader (SpectraMax 340; Molecular Devices, Inc.).

Quantitative determination of type I collagen secretion. Type I collagen secretion was assessed using a pro-collagen type 1 C-peptide (PIP) enzyme immunoassay (MK101; Takara Bio Inc.). Briefly, NHDFs were plated into microtiter plates (96 wells) at a density of $1x10^5$ cells/well, serum-starved for 24 h, and incubated with NK-CdM at concentrations of 2.5, 5, and 10% for 48 h. TGF-β (10 nM) was employed as a positive control. After the incubation period, 100 µl an antibody-peroxidase conjugate solution was added to each well, followed by the addition of 20 µl diluents or standard solution. After incubation for 3 h at 37˚C, the well contents were removed by aspiration, and all the wells were washed four times with 400 µl PBS. Following this, 100 µl substrate solution was added to each well and the plates were incubated at room temperature for 15 min. The reaction was stopped by the addition of 100 µl stop solution. Absorbance was measured at 450 nm using an ELISA reader (SpectraMax 340; Molecular Devices, LLC).

MMP-1 inhibition assay. MMP-1 activity was determined using an MMP-1 immunoassay kit (DY901; R&D Systems, Inc.). NHDFs were seeded in microtiter plates (96 wells) at a density of $1x10^5$ cells per well. The cells were pretreated, serum starved for 24 h, and then treated with NK-CdM prior to UV-B irradiation (30 mJ/cm^2) using a Biospectra (Vilber Lourmat) and harvested after 48 h. Before UV-B irradiation, the cultures were rinsed with PBS and irradiated at the indicated intensity in PBS to avoid absorption by the phenol-red present in the culture medium. All cell treatment groups were similarly cultured in PBS at room temperature during the experimental procedure to ensure equal treatment conditions. The activity of MMP-1 in the cell supernatant was determined using the method described in the MMP-1 assay kit.

Quantification of elastin. Supernatants from NHDF cultures were collected, serum starved for 24 h, and then treated with NK-CdM for 48 h. Supernatants were analyzed using the Fastin Elastin Assay kit (Biocolor Ltd.) as recommended by the manufacturer. The Fastin Elastin Assay uses a dye reagent

Table I. Primer sequence information used in reverse transcription-quantitative PCR.

Gene	Sequences
Type 1 collagen	
Forward	5'-AGACTGGCAACCTCAAGAAG-3'
Reverse	5'-TTCGGTTGGTCAAAGATAAA-3'
Type 3 collagen	
Forward	5'-ATGGTTGCACGAAACACACT-3'
Reverse	5'-CTTGATCAGGACCACCAATG-3'
MMP-1	
Forward	5'-CTGGCCACAACTGCCAAAT-3'
Reverse	5'-CTGTCCCTGAACAGCCCAGTACTTA-3'
MMP-2	
Forward	5'-TCTCCTGACATTGACCTTGGC-3'
Reverse	5'-CAAGGTGCTGGCTGAGTAGATC-3'
MMP-3	
Forward	5'-ACACCGGATCTGCCAAGAGA-3'
Reverse	5'-CTGGAGAACGTGAGTGGAGTCA-3'
MMP-9	
Forward	5'-TTGACAGCGACAAGAAGTGG-3'
Reverse	5'-GCCATTCACGTCGTCCTTAT-3'
TIMP-1	
Forward	5'-TCTGCAATTCCGACCTCGTCATCA-3'
Reverse	5'-AAGGTGGTCTGGTTGACTTCTGGT-3'
Tropoelastin	
Forward	5'-CGGAATTCACCTCTTAAGCCAGTTCCCG-3'
Reverse	5'-CCCAAGCTTCGGGAACACCTCCGACACTA-3'
GAPDH	
Forward	5'-AGGGCTGCTTTTAACTCTGGT-3'
Reverse	5'-CCCCACTTGATTTTGGAGGGA-3'

MMP, matrix metalloproteinase; TIMP, tissue inhibitor of metalloproteinase.

that binds to the 'basic' and 'non-polar' amino acid sequences found in mammalian elastins. The recovered dye-bound elastins from each sample and the standards were detected by reading the absorption at 513 nm. All measurements were performed in triplicate. The measured amount of each elastin protein was normalized to the corresponding cell number.

Antibody array. Growth factor levels in the NK-CdM were assessed using an antibody array kit (C1; RayBiotech) according to the manufacturer's protocol. Unconditioned NK cell medium was used as the negative control. The membranes were blocked by incubation with the blocking buffer at room temperature for 30 min and incubated with the sample at room temperature for 3 h. Membranes were then washed three times with Wash Buffer I and two times with Wash Buffer II at room temperature for 5 min per wash and incubated with biotin-conjugated antibodies at room temperature for 2 h. Finally, the membranes were washed, incubated with HRP conjugated streptavidin at room temperature for 2 h and with detection buffer for 1 min, and exposed to X-ray film for 40 sec (Kodak). The exposed films were digitized and the relative growth factor levels were compared after densitometry analysis (Scion NIH Image 1.63). The relative protein levels were obtained by subtracting the background staining and normalizing to the positive controls on the same membrane.

RNA isolation and reverse transcription-quantitative polymerase chain reaction (RT-qPCR) analysis. Total RNA was extracted from the dorsal skin tissues and isolated using the Trizol® reagent (Invitrogen; Thermo Fisher Scientific, Inc.) according to the manufacturer's protocol cDNA synthesis was performed according to the protocol provided by the Takara PrimeScript™ RT Master Mix (Takara Bio, Inc.). The temperature protocol for RT was as follows: 37˚C for 15 min, followed by 85˚C for 5 sec. For quantitative PCR, TB Green® Premix Ex Taq™ II (Takara Bio, Inc.) and CFX96TM Real-Time System (Bio-Rad Laboratories, Inc.) were used, and all reactions were repeated three times under the following conditions: Initial denaturation at 95˚C for 30 sec, followed by 40 cycles at 95˚C for 5 sec and 60˚C for 30 sec. Relative gene expression values were determined using the $2^{-\Delta\Delta Cq}$ method (23). The primers used for q-PCR are listed in Table I.

Western blot analysis. The harvested tissues were homogenized in Pro-prep solution (iNtRON Biotechnology) and lysates were centrifuged at 12,000 x g for 30 min at 4˚C. Total protein (40 μg) was separated by electrophoresis on 6-8% SDS-polyacrylamide gels and transferred to polyvinylidene fluoride membranes (EMD Millipore). After transfer, the membranes were blocked with 5% fat-free milk-TBST buffer for 1 h at room temperature and washed with TBS containing 0.05% Tween-20 (TBS-T). The membranes were incubated overnight at 4˚C with a 1:1,000 dilution of primary rabbit monoclonal antibodies against proCOL1A1 (Santa Cruz Biotechnology, Inc.; cat. no. sc-30136), collagen type I (Novus Biologicals, LLC; cat. no. NB600-408), MMP-3 (Abcam; cat. no. ab52915), TIMP-1 [Cell Signaling Technology, Inc. (CST); cat. no. 8946], phospho-p38 (CST; cat. no. 4511), phospho-c-Fos (CST; cat. no. 5348), c-Fos (CST; cat. no. 2250), primary rabbit polyclonal antibodies against collagen type III (Abcam; cat. no. ab7778), α-elastin (Abcam; cat. no. ab21607), MMP-1 (Abcam, cat. no. ab137332), MMP-2 (CST; cat. no. 4022), MMP-9 (Abcam; cat. no. ab38898), p38 (CST; cat. no. 9212), phospho-ERK (CST; cat. no. 9101), ERK (CST; cat.no.9102), phospho-JNK (CST; cat.no.9251), JNK (CST; cat. no. 9252), phospho-c-Jun (CST; cat. no. 9164), c-Jun (CST; cat. no. 9165), and mouse monoclonal antibodies against β-actin (Santa Cruz Biotechnology, Inc.; cat. no. sc-47778). For pathway determination, the following inhibitors were added and incubated for 30 min at 37˚C: 20 μM of PD98059 (ERK inhibitor; cat. no. 167869-21-8; EMD Millipore), 20 μM of SP600125 (JNK inhibitor; cat. no. 129-56-6; EMD Millipore), 15 μM of SB203580 (p38 inhibitor; cat. no. 152121-47-6; EMD Millipore), 20 μM of LY294002 (PI3K inhibitor, cat. no. 942289-87-4; EMD Millipore). Samples were then treated with 1.25% NK-CdM. After washing the blots three times with TBST, bound primary antibodies were detected by the addition of HRP-conjugated anti-mouse (1:1,000; cat. no. P0447; Dako; Agilent Technologies, Inc.) or anti-rabbit secondary antibodies (1:1,000; cat. no. P0448; Dako; Agilent Technologies, Inc.) for 1 h at room temperature. The transferred proteins were visualized with a Pierce ECL western blotting substrate (Thermo Fisher Scientific, Inc.) and quantified by scanning densitometry using Image-Pro Plus 6.0 (Media Cybernetics, Inc.).

Total antioxidant capacity assay. An antioxidant assay (709001; Cayman Chemical Company) based on the oxidation of 2,2'-azino-di-(3-ethylbenzthiazoline sulfonate), was used to measure the total antioxidant capacity according to the manufacturer's protocol. Values were compared to a standard curve of known concentrations of Trolox (a tocopherol/vitamin E antioxidant analogue).

Immunocytochemistry. NHDFs were seeded into a chamber slide, serum starved for 24 h, and then treated with NK-CdM for 48 h. Following treatment with 4% paraformaldehyde for 10 min at 4˚C and 0.1% Triton X-100 for 5 min, the cultured NHDFs were incubated with an anti-type I collagen antibody (1:500; cat. no. ab34710; Abcam) at 4˚C overnight and then with fluorescein isothiocyanate-labeled goat anti-rabbit IgG (1:1,000; cat. no. NB7182; Novus Biologicals, LLC). A 4'6-diamidino-2-phenylindole mounting medium kit (OriGene Technologies, Inc.) was used to counterstain the nuclei for 10 min at room temperature, and stained cells were visualized using an Olympus FLUOVIEW FV10i confocal microscope (Olympus Optical Co., Ltd.).

3D reconstructed human full skin model (Keraskin-FT™) and UV-B irradiation. A Keraskin-FT™ and Keraskin-FT™ culture media were purchased from Biosolution Co., Ltd. After shipment, the tissues were transferred into 6-well plates filled with 0.9 ml culture media per well, and pre-incubated at 37˚C in 5% CO_2 for 24 h. The tissues were irradiated with UV-B (125 mJ/cm^2) and then test materials were applied to the surface of the insert with NK-CdM (50 and 100%) diluted in PBS containing 0.1% DMSO for 48 h. The culture medium and tissues were recovered for analysis using ELISA kits for Pro-collagen type 1 C-peptide (PIP) enzyme immunoassay (cat. no. MK101; Takara Bio, Inc.) and MMP-1 immunoassay kits (cat. no. DY901; R&D Systems, Inc.) and picrosirius red staining, respectively.

Picrosirius red staining. The KeraSkin™-FT model (Biosolution) was fixed with 4% formaldehyde for 10 min at 4˚C, embedded with paraffin, and prepared as 4 μm sections using a microtome (Leica Microsystems, Inc.). Paraffin sections were de-paraffinized in xylene, hydrated through a decreasing ethanol concentration, and fixed with Bouin's solution for 1 h at room temperature. The sections were counterstained with 0.1% Fast Green in distilled water for 10 min at room temperature, and collagen was stained using 0.1% Sirius red in saturated aqueous picric acid for 30 min at room temperature. After dehydration and mounting, the tissues were examined under a microscope (Olympus Corporation). Each pathologist assigned each section a score according to the following scale: 0=negative control, +=moderately increased staining, ++=considerably increased staining), based on the percentage of stained cells in each category.

Statistical analyses. Statistical analyses of data were performed using the Student's t-test or multivariate analysis of variance by post hoc Tukey method for direct comparison. Data were analyzed using SPSS software version 12.0 (SPSS, Inc.). The results are expressed as the mean ± standard deviation of at least three independent experiments. $P<0.05$ was considered to indicate a statistically significant difference.

Results

Detection of active biomolecules in the conditioned medium derived from NK cells. The growth factors present in NK-CdM were first profiled using a human growth factor antibody array capable of detecting 41 growth factors. A map of the array is shown in Fig. 1A. Compared with the NK culture medium, NK-CdM showed a strong increase in the levels of five individual growth factors. These were granulocyte-macrophage colony-stimulating factor (GM-CSF), insulin-like growth factor binding protein 2 (IGFBP), macrophage colony-stimulating factor (M-CSF), platelet-derived growth factor-AA (PDGF-AA), and TGF-β2 (Fig. 1B).

Effect of NK-CdM on proliferation and collagen synthesis in NHDFs. Next, the effects of NK-CdM on NHDF proliferation and their ability to synthesize collagen were evaluated.

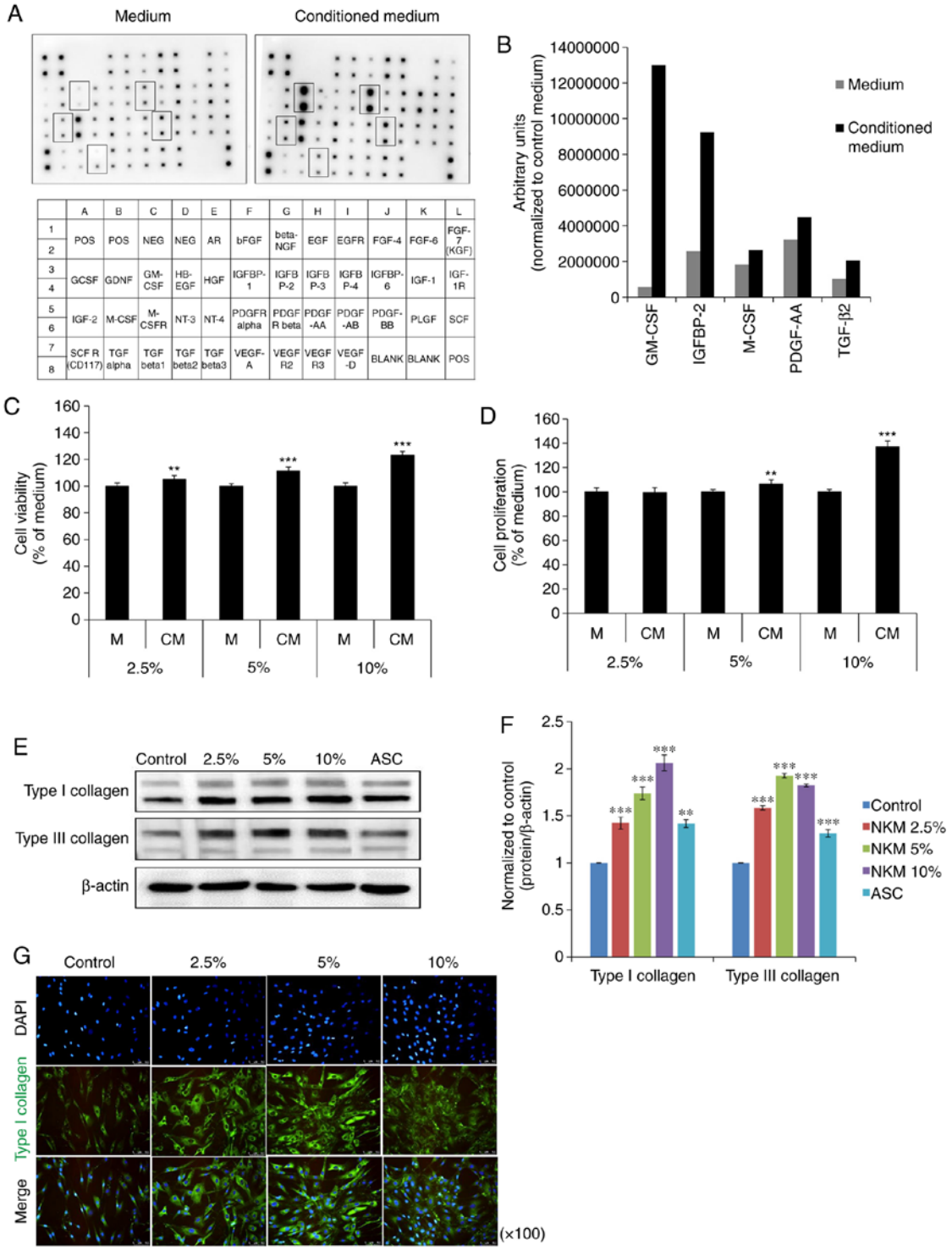

Figure 1. Impact of NK-CdM on NHDF growth and collagen synthesis. Growth factor array analysis of NK-CdM. (A) List of growth factors on the array membrane (lower panel) with significantly detected growth factors marked (upper panel). (B) Growth factor secretion profiles of NK-CdM. A human growth factor antibody array was used to detect paracrine factors present in NK-CdM. (C) Proliferation of NHDFs treated with NK-CdM at various concentrations for 24 h. (D) Time course of NHDF proliferation up to 72 h. Data are shown as the mean ± standard deviation of three independent experiments. (E) Western blotting and (F) graphical representation of the effects of NK-CdM on collagen synthesis in NHDFs. NHDFs were treated with medium (Control), ASC, (200 μM), or NK-CdM (2.5, 5 and 10%) for 72 h and the expression of type I collagen and type III collagen was measured by western blot analysis and normalized to the expression of β-actin. (G) Immunocytochemical analysis showing the activation of type I collagen in NK-CdM-treated NHDFs. NHDFs were fixed and then incubated with a goat anti-rabbit type I collagen antibody. Type I collagen staining was detected with a fluorescein isothiocyanate conjugated anti-goat IgG antibody by fluorescence microscopy. Magnification, x100. **P<0.01 and ***P<0.001 vs. control. NK-CdM, natural killer cell conditioned medium; NHDF, neonatal human dermal fibroblasts; ASC, ascorbic acid.

Treatment of NHDFs with NK-CdM (2.5, 5 and 10%) for up to 24 h did not induce cell toxicity (Fig. 1C). At 72 h, the cell viability increased in a concentration-dependent manner. The ability of NK-CdM to increase NHDF proliferation was measured at 24 and 72 h using a CCK-8 assay. At 24 h, NK-CdM caused a dose-dependent increase in NHDF

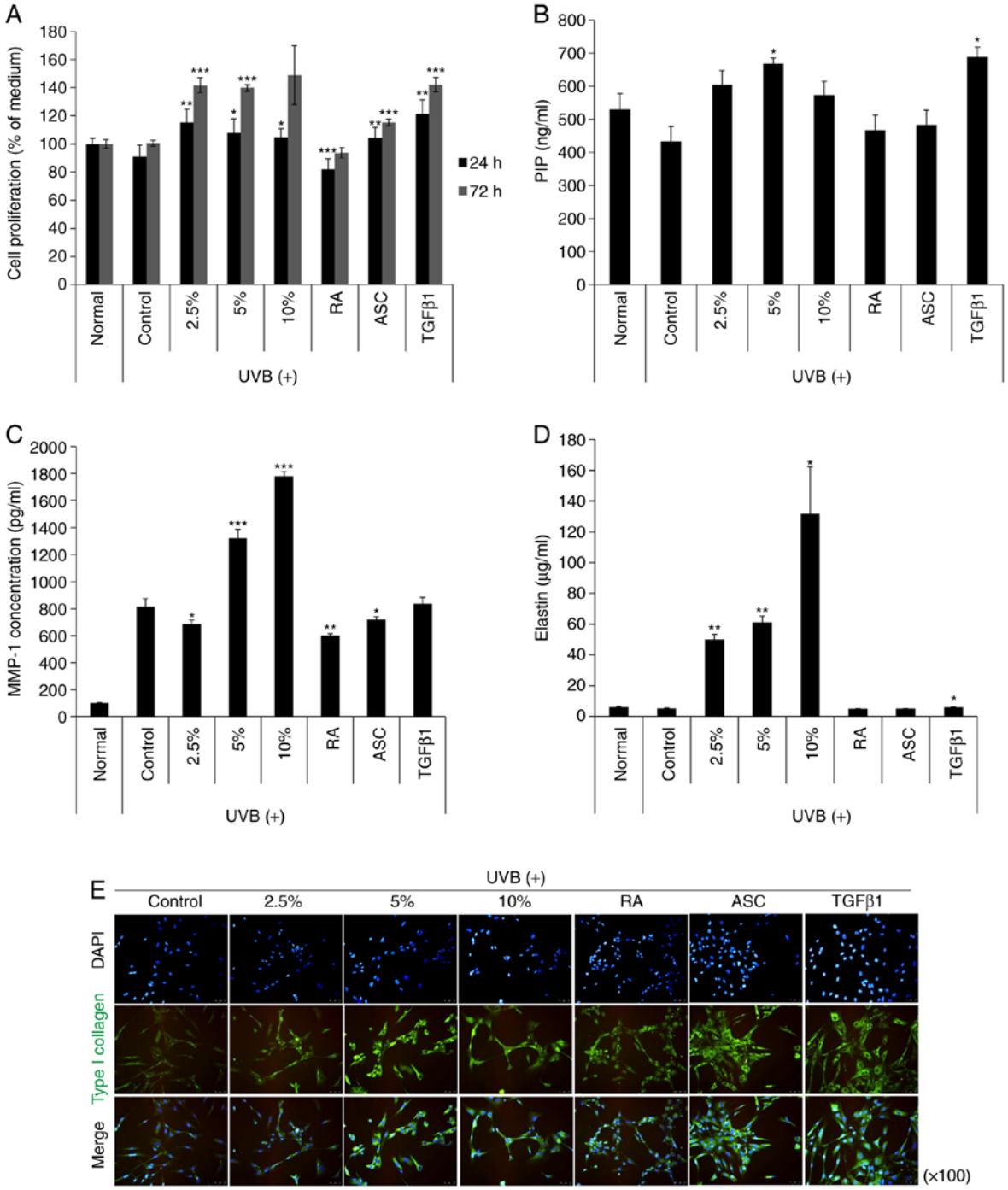

Figure 2. The effects of NK-CdM on UV-B-induced MMP-1 and type I procollagen secretion in NHDFs. NHDFs were irradiated with 30 mJ/cm^2 UV-B, followed by treatment with the indicated concentrations of NK-CdM (2.5, 5 and 10%), RA (0.03 μg/ml), ASC (200 μM), and TGF-β1 (10 ng/ml). (A) Time course of NHDF proliferation up to 24 and 72 h. (B) PIP secretion, (C) MMP-1 levels, and (D) Elastin levels in harvesting culture media at 48 h. MMP-1, PIP, and elastin levels were measured using a commercially available ELISA kit, as described in the Methods section. The data are the mean ± standard deviation values of three individual experiments. (E) Immunocytochemical analysis showing an inhibition of type 1 collagen induction in NK-CdM-treated NHDF cells. Magnification, x100. *P<0.05, **P<0.01 and ***P<0.001 vs. Control (UV-B only group). MMP, matrix metalloproteinase; PIP, pro-collagen type 1 C-peptide; NK-CdM, natural killer cell conditioned medium; NHDF, neonatal human dermal fibroblasts; UV, ultraviolet; RA, retinoic acid; ASC, ascorbic acid; TGF, transforming growth factor.

proliferation, with a maximal increase of 1.37-fold observed at 10% NK-CdM (Fig. 1D). The expression levels of proteins related to collagen synthesis were also analyzed by western blotting. NHDFs were treated with NK-CdM (2.5, 5 and 10%) for 48 h, using ascorbic acid (200 μM) as the positive control. The expression of type I collagen and type III collagen was increased in a dose-dependent manner in NK-CdM treated cells (Fig. 1E and F). Fig. 1G shows that both intracellular collagen production and extracellular collagen secretion levels were increased after 48 h of treatment with NK-CdM. Therefore, NK-CdM increases both type I collagen production and proliferation in NHDFs.

NK-CdM inhibits the collagen degradation induced by UV-B irradiation of NDHFs. Next, the effect of NK-CdM treatment (2.5, 5 and 10%) on proliferation in UV-B treated NK-CdM

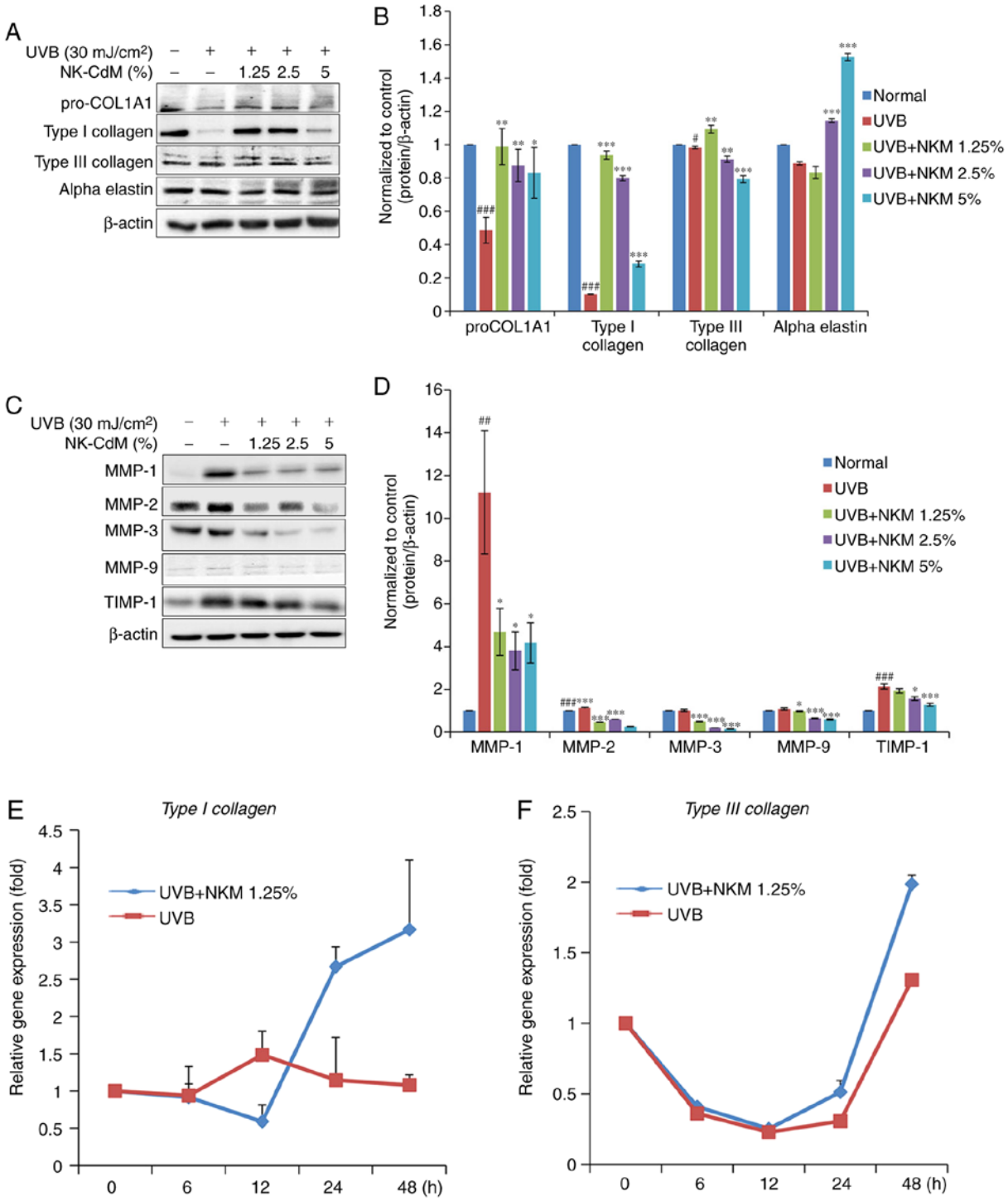

Figure 3. Modulation of the expression of MMPs/collagen in UV-B-irradiated NHDFs by NK-CdM. After being serum-starved for 24 h, NHDFs were irradiated with UV-B (30 mJ/cm^2), and further incubated with NK-CdM at the indicated concentrations for 48 h. (A) The expression levels of procollagen I, type I collagen, type III collagen, α-elastin and (B) a quantitative densitometric analysis of the upper bands. (C) MMP-1, -2, -3, -9, and TIMP-1 were evaluated by western blotting. (D) The bar graph (mean ± standard deviation of the mean; n=3) represent a quantitative densitometric analysis of the upper bands. Changes in the mRNA expression of (E) type I collagen and (F) type III collagen were determined using quantitative PCR at 0, 6, 12, 24 and 48 h following culture in NK-CdM after UV-B exposure.

cells was evaluated. As a result, the cytotoxicity induced by UV-B exposure was reduced over time (Fig. 2A). Next, to investigate the effect of NK-CdM on collagen synthesis and/or secretion by NHDF cells, the amount of PIP was measured in the culture supernatants of NHDF cells treated with NK-CdM after UV-B irradiation. As shown in Fig. 2B, NHDF cells treated with 2.5% NK-CdM effectively produced PIP compared with the TGF-β1 treated group. In addition, the effect of NK-CdM on UV-B-induced MMP-1 secretion was also determined. The PIP levels in the culture supernatants accumulated significantly within 48 h after the addition of 5% NK-CdM ($P<0.05$), with the MMP-1 levels decreased by 2.5% NK-CdM ($P<0.05$). Moreover, treatment with NK-CdM significantly stimulated elastin synthesis in a dose-dependent

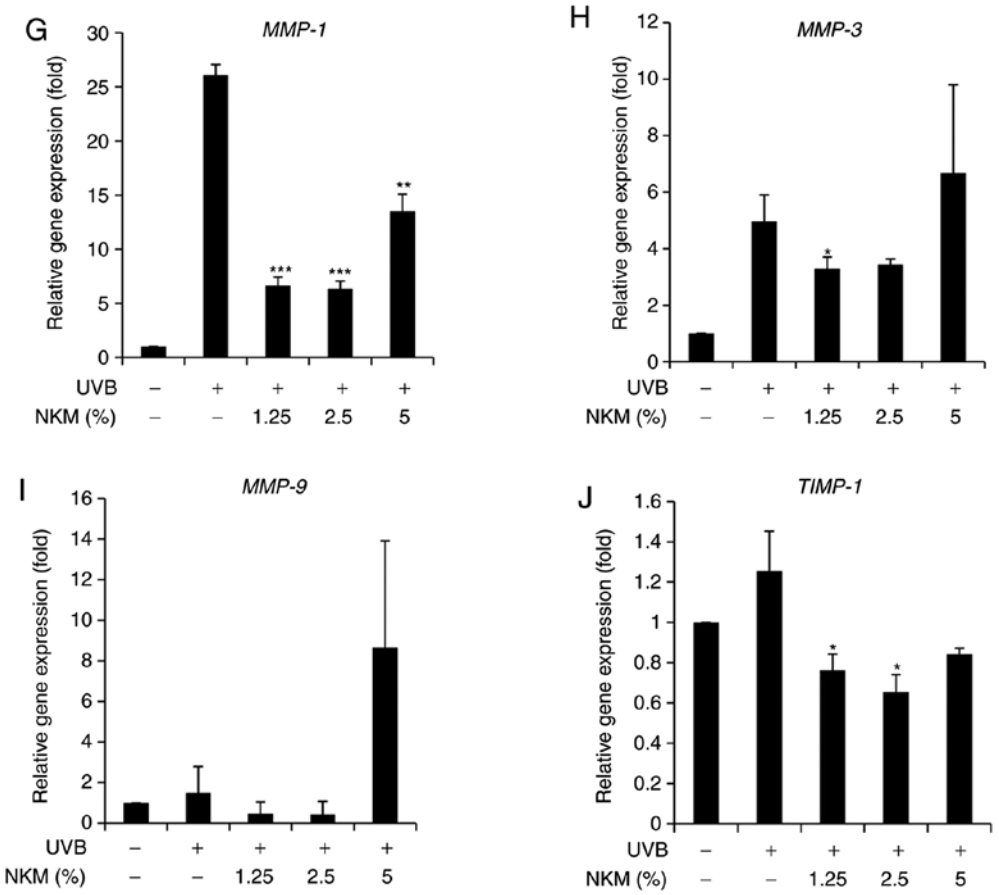

Figure 3. Continued. The expression of photoaging-related genes such as (G) MMP-1, (H) MMP-3, (I) MMP-9, and (J) TIMP-1 was evaluated by quantitative PCR. Equal protein and mRNA loading were verified by normalization with β-actin and GAPDH, respectively. *P<0.05, **P<0.01 and ***P<0.001 vs. with the UV-B-irradiated control. $^{\#}$P<0.05, $^{\#\#}$P<0.01 and $^{\#\#\#}$P<0.001 vs. the Normal (non-irradiated control). MMP, matrix metalloproteinase; NK-CdM, natural killer cell conditioned medium; NHDF, neonatal human dermal fibroblasts; UV, ultraviolet; TGF, transforming growth factor; TIMP, tissue inhibitor of matrix metalloproteinases.

manner, whereas the other group did not (P<0.05; Fig. 2D). However, measuring the protein expression level of elastin is not sufficient to examine the level of elastin deposition in the ECM. Changes in intracellular type collagen I expression levels were detected by immunofluorescent staining. After 48 h of NK-CdM treatment (2.5, 5 and 10%), NHDF cells showed a markedly increased level of type I collagen compared to that in untreated cells, and NK-CdM was also effective in increasing the recovery of the expression of type I collagen after UV-B irradiation (Fig. 2E). However, quantitative determination of type I collagen secretion does not indicate deposition of collagen. These results demonstrate that NK-CdM treatment increases both total collagen and type I procollagen secretion, as well as total elastin synthesis.

NK-CdM inhibits UV-B-induced collagen degradation via inactivation of ROS/JNK signaling in NHDFs. The effect of UV-B treatment on the expression of collagen and MMP family members in NHDFs was examined by both western blot analysis and RT-qPCR. The western blot analysis indicated that UV-B irradiation of NHDF cells increased the levels of MMPs and decreased collagen expression. NK-CdM treatment (1.25-5%) completely blocked the upregulation of MMPs and promoted collagen synthesis, essentially reversing the effects of UV-B irradiation (Fig. 3A-D). RT-qPCR analysis revealed that UV-B-irradiation decreased the levels of mRNAs encoding type I collagen and type III collagen in NHDFs and that treatment with NK-CdM enhanced the levels of these collagens in a time- and dose-dependent manner (Fig. 3E and F). In addition, the mRNA expression levels of MMP-1, MMP-3, MMP-9, TIMP-1 were markedly increased in UV-B-exposed NHDF cells, but these increases were inhibited by treatment with 1.25% NK-CdM for 48 h. However, these increases were not dose-dependently inhibited (Fig. 3E).

To further understand the molecular mechanisms underlying these effects of NK-CdM in UV-B-exposed NHDF cells, the effect of NK-CdM on c-Jun phosphorylation levels and c-Fos expression levels was examined. Since AP-1 is activated by MAPK signaling, the effects of NK-CdM on the different MAPK signaling pathways were studied further in UV-B-irradiated NHDFs. As shown in Fig. 4, UV-B radiation elevated the phosphorylation of the different MAPK molecules namely, ERK, JNK, and p38. Interestingly, NK-CdM treatment was found to partially inhibit the phosphorylation of ERK, JNK, and p38 induced by UV-B exposure, respectively. It was confirmed that 1.25% NK-CdM recovered UV-aB-induced decrease in collagen. Based on these results, inhibition experiments were performed using 1.25% NK-CdM; it was not necessary to conduct experiments with increasing concentrations of inhibitors.

As shown in Fig. 4, UV-B irradiation increased c-Jun phosphorylation levels as well as c-Fos expression levels in NHDFs.

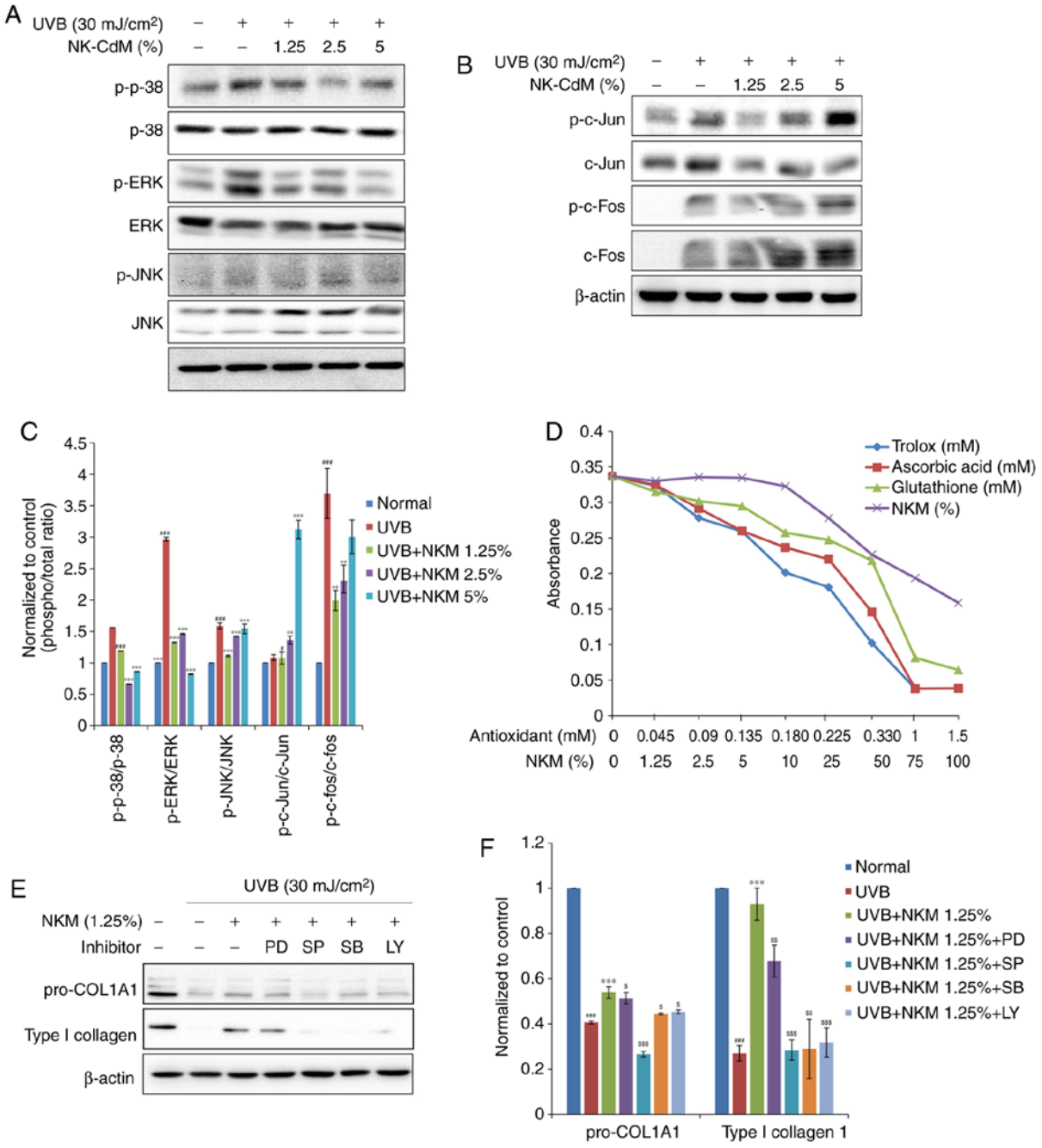

Figure 4. Inhibitory effect of the phosphorylation of the JNK, p38 MAPK, and ERK1/2, and the transcription factors c-Jun and c-Fos, in UV-B-exposed and NK-CdM-treated NHDFs. After being serum-starved for 24 h, NHDFs were irradiated with UV-B (30 mJ/cm^2), and further incubated with NK-CdM at the indicated concentrations for 48 h. Total cell protein extracts were prepared and separated by electrophoresis on SDS-PAGE gels followed by a western blot analysis with primary antibodies capable of detecting (A) phospho-JNK, -p38 MAPK, and -ERK1/2 and (B) phospho-c-Jun, -c-Fos. β-actin was used as the loading control. (C) Equal protein loading was verified by analyzing β-actin levels. (D) The antioxidant activity of NK-CdM, at the indicated concentration, was measured using an Antioxidant Assay kit. (E) NHDFs were treated with 10 μM of the ERK1/2 inhibitor PD, 10 μM of the JNK inhibitor SP, 10 μM of the p38 MAPK inhibitor SB, or 10 μM of the PI3K inhibitor LY and then irradiated. The levels of procollagen I and type I collagen at 48 h after irradiation were measured by western blot analysis. (F) The bar graphs (mean ± standard error of the mean; n=3) represent a quantitative densitometric analysis of the bands. $^{\#}$P<0.05 and $^{\#\#\#}$P<0.001 vs. the Normal (non-irradiated control). **P<0.01 and ***P<0.001 vs. the UV-B-irradiated control. $^{\$}$P<0.05, $^{\$\$}$P<0.01 and $^{\$\$\$}$P<0.001 vs. the UV-B irradiated and 1.25% NK-CdM treated group. MMP, matrix metalloproteinase; ERK, extracellular signal regulated kinase; NK-CdM, natural killer cell conditioned medium; NHDF, neonatal human dermal fibroblasts; UV, ultraviolet; MAPK, mitogen associated protein kinase; PI3K, phosphatidylinositol 3 kinase; SP, SP600125; LY, LY294002; SB, SB203580; PD, PD98059; phosphor, phosphorylated; JNK, c-Jun N terminal kinase.

The upregulation of c-Jun phosphorylation observed after UV-B exposure was not dose-dependently reduced by NK-CdM treatment (Fig. 4B).

The antioxidant activity of NK-CdM was also directly measured using an antioxidant assay kit. The antioxidative capacity of NK-CdM, expressed relative to the antioxidative capacity of Trolox, increased in a dose-dependent manner (Fig. 4D). Interestingly, NK-CdM (>50%) had a similar antioxidative effect to that of glutathione (0.33 mM).

Next, PD98059 (an ERK inhibitor), SP600125 (a JNK inhibitor), SB203580 (a p38 inhibitor), and LY294002 (a PI3K inhibitor) were used to further investigate the activation

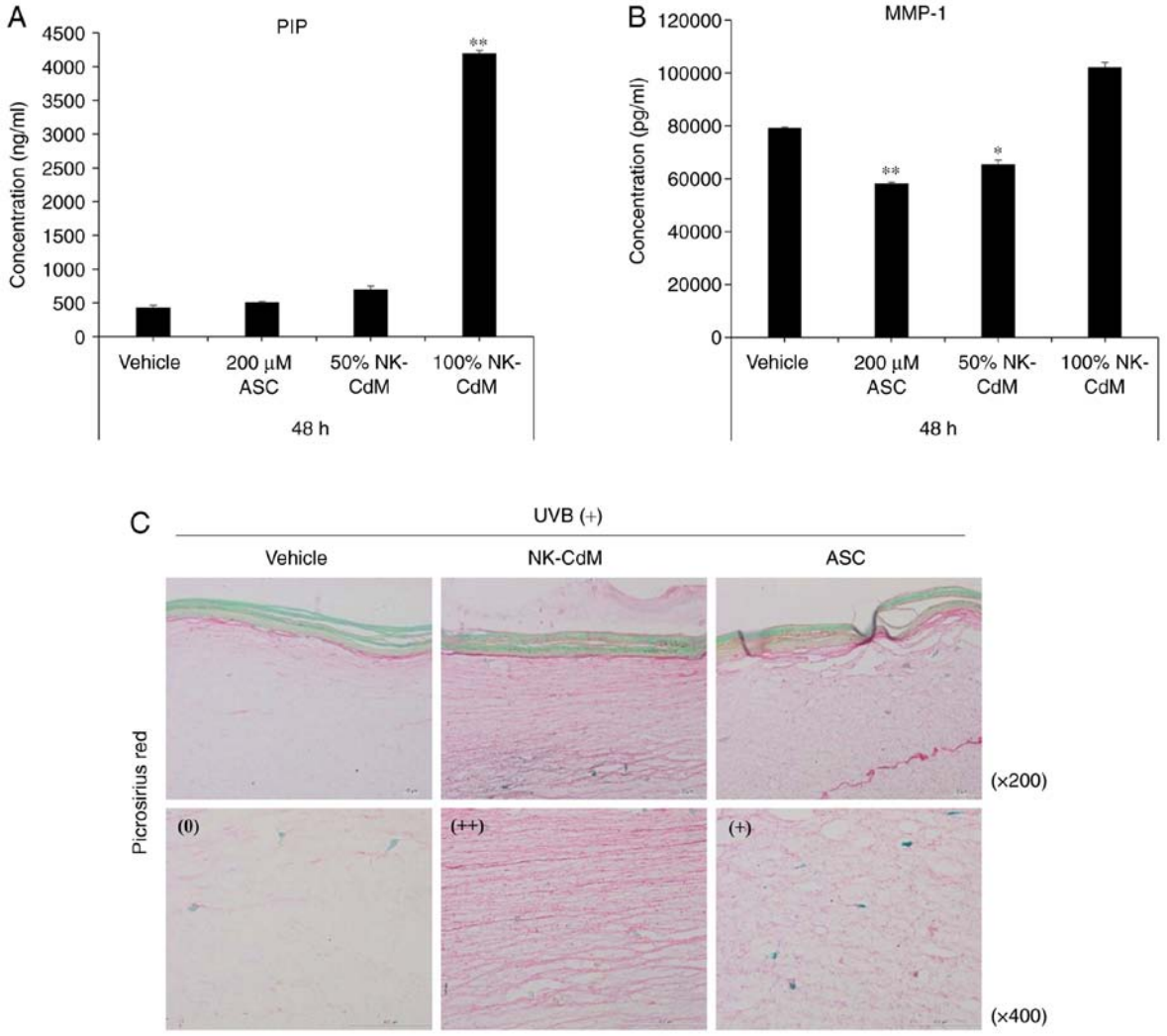

Figure 5. Inhibitory effects of NK-CdM on UV-B-induced collagen degradation in a 3D reconstructed human full skin model. Tissues were irradiated with UV-B (125 mJ/cm^2), and further incubated with vehicle (PBS containing 0.1% DMSO) and NK-CdM (50 and 100%) and ascorbic acid (200 μM) at the indicated concentrations for 48 h. The levels of (A) type I procollagen and (B) MMP-1 in the culture media were measured using a commercially available ELISA kit, as described in the Methods. The data are the mean ± standard deviation values of three individual experiments. *P<0.05 and **P<0.01 vs. UV-B-irradiated vehicle control. (C) To confirm the inhibitory effects of NK-CdM on UV-B-induced collagen degradation in skin model, the Keraskin-FT™ was stained with PSR, which stains collagen red. The visual assessments of collagen degradation represent the average of the scores in each PSR staining intensity category (++ indicates pronounced findings, + moderate findings, and 0 no/scant findings) identified for each score. NK-CdM, natural killer cell conditioned medium; NHDF, neonatal human dermal fibroblasts; UV, ultraviolet; PSR, picrosirius red; ASC, ascorbic acid; MMP, matrix metalloproteinase; PIP, pro-collagen type 1 C-peptide.

of the different MAPK pathways. Consistently, SP600125, SB203580, and LY294002, but not PD98059, partially blocked the NK-CdM-induced increase in collagen levels (Fig. 4E). Taken together, these results suggest that NK-CdM has an antioxidative activity, protecting NHDFs by scavenging free radicals and reducing UV-B-induced MMP-1 and type I collagen expression by modulating the ROS-mediated JNK signaling pathway.

Effects of NK-CdM on UV-B-induced photoaging in a 3D reconstructed human full skin model. To further assess the effects of NK-CdM on collagen production after exposure to UV-B, type I collagen expression was examined in the biopsied tissue irradiated with UV-B. As shown in Fig. 5A and B, the UV-B-induced increases in MMP-1 expression and secretion were inhibited by treatment with NK-CdM (50 and 100%) for 48 h, while at the same time, NK-CdM caused a dramatic increase in collagen-1 levels. To visually examine the anti-photoaging effects of NK-CdM, UV-B-treated Keraskin-FT™ sections were stained with a picrosirius red stain. As a result, NK-CdM treatment increased the diameter of the collagen fibers (Fig. 5C). Therefore, the various growth factors present in NK-CdM appear to cause the proliferation of fibroblasts and the production of ECM, resulting in the formation of thick mature collagen.

Discussion

Conditioned medium (CM) from various sources, containing numerous growth factors and cytokines, is known to promote the regeneration of damaged tissue and so might be of use in regenerating aged skin (24). Growth factors present in CM could reduce the signs of skin aging as a result of their ability to stimulate the proliferation of dermal fibroblasts and keratinocytes and induce the production of extracellular matrix components, including collagen (17). Therefore, NK-CdM can

stimulate both collagen synthesis and the migration of fibroblasts during the wound healing process and so is of potential utility in regenerating aged skin.

The antibody array results were compared between unconditioned NK cell media and conditioned NK cell media. For the remaining experiments, diluted NK-CdM was used for treating fibroblasts. This experiment was aimed to characterize NK-CdM, and it was confirmed that no specific cytokine and growth factor were generated in Medium 106, a free medium for fibroblasts. The present study found that NK-CdM contains factors that are anti-apoptotic such as IGFBP, GM-CSF, SCF; angiogenic such as VEGF; anti-inflammatory such as TGFβ; and also factors that promote proliferation and migration of progenitor cells such as IGF-1, PDGF, and GM-CSF. Interestingly, TGF-β appears to modulate the action of growth factors on the expression of MMPs and TIMPs (25). Thus, TGF-β and PDGF are important players in maintaining the proper balance between the tissue modification and repair processes that involve many cytokines (26). Kim *et al* (27) also reported that the effect PDGF-AA on the production of type I collagen in human fibroblasts, suggesting its function as a key factor in skin remodeling and skin aging.

Type I collagen is the most abundant protein found in skin connective tissue and along with other types of collagen (III, V and VII), elastin, proteoglycans, fibronectin, and other ECM proteins, it helps maintain the skin structure (28). Fibrous (type I and III) collagen is characteristic of chronologically aged or damaged skin. Type I collagen levels are regulated by the activity of MMPs, a family of zinc-requiring endoproteases that can degrade all the components of the ECM. Of particular importance, MMP-1 initiates the degradation of collagen type I and III, whereas MMP-9 further degrades the collagen fragments produced by MMP-1 (29). All of the known MMPs are inhibited by the four homologous TIMP proteins. Of particular importance, TIMP-2 inhibits ECM proteolysis in a number of tissues by directly inhibiting the activity of metalloproteinases, including MMP-2. TIMP-2 is also known to be required for the activation of MMP-2. In this study, NK-CdM inhibited the expression of MMP-1, as well as MMP-2 and MMP-9, in NHDFs. Moreover, the expression of TIMP-2 was generally increased by NK-CdM treatment. Overall, these results suggest that the increased levels of type I procollagen induced by NK-CdM in UV-B treated NHDFs may be caused by a decrease in MMP-1, MMP-2, and MMP-9 expression/activity levels and an increase in TIMP-2 levels. At the mRNA level, low-levels of the mRNA encoding MMP-9 were detected, but MMP-9 expression levels were considerably changed. Treatment with NK-CdM inhibited the mRNA expression of MMP-9. When high concentration of medium is directly applied to the cells, various growth factors and cytokines are secreted in excess, thereby inhibiting cell proliferation. Although it may be used without dilution, toxicity due to the substance itself may appear at a high concentration; even if it is not toxic, it may not be cost effective. Therefore, the experiment was carried out by diluting NK-CdM, in order to confirm that it is effective at low concentrations.

When UV-A and UV-B are applied to the skin, UV-A acts on the dermis while UV-B acts directly on the epidermis. The penetration of UV-B into the dermis is limited by its wavelength. Since UV-A penetrates deeper, it seems to be more important. Although their targets are different, both UV-A and UV-B generate ROS, and the mechanism of photoaging is the same for both. Moreover, UV-B has a lower penetration rate into the dermis owing to its shorter wavelength than UV-A; however, its energy is stronger than that of UV-A, which is more suitable for visualizing the photoaging mechanism of ROS.

Excessive production of ROS, induced by UV-B radiation, may be the cause of UV-B-induced toxicity (30). Therefore, the use of antioxidants that interfere with ROS production may be preferable for the prevention of photoaging and skin cancer. ROS also plays an important role in collagen metabolism (31). ROS not only directly destroys collagen, but also inactivates TIMPs, while at the same time inducing the synthesis and activation of matrix-degrading metalloproteases.

In addition to increasing MMP production and decreasing collagen levels, UV irradiation also reduces the expression of TGF-β2 (32). Since TGF-β2 promotes collagen formation, a decrease in its expression levels also leads to a reduction in collagen production. As described earlier, UV light exposure and the subsequent generation of ROS result in the decreased synthesis of collagens type I and III and an increase in MMP-1 activity in the dermis. Oxidative stress induces the phosphorylation of proteins in the different MAPK signaling pathways, namely, ERK, JNK, and p38, as well as the activation of the protein kinase B pathway (33). In this study, the UV-B-induced phosphorylation of ERK, JNK, and p38 was attenuated by NK-CdM treatment. Since the activation of JNK phosphorylates c-Jun to increase AP-1 complex transcriptional activity, NK-CdM appears to inhibit UV-B-induced AP-1 activation by reducing c-Jun phosphorylation and c-Fos expression, thereby reducing MMP-1 levels.

3D reconstructed human tissue models are widely used to examine the effects of cosmetic ingredients and their safety in an *in vivo*-like condition (34). In the present study, the anti-aging effects of NK-CdM were also examined using a 3D reconstructed human skin model. It was observed that similar to the NHDFs, UV irradiation decreased collagen levels and increased MMP levels, and this could be prevented by NK-CdM. Importantly, to confirm that NK-CdM prevents UV-B-induced photoaging, NK-CdM was treated at different concentrations and the effect was confirmed at low concentrations. Therefore, the present study concluded that there is a relationship between the biological effect and the NK-CdM concentration used to confirm its various effects.

The present study demonstrates that NK-CdM inhibits UV-B-induced MMP expression. The mechanisms underlying the anti-photoaging effect of NK-CdM involve its actions on UV-B-induced ROS generation and inhibition of MAPK activation. Therefore, the authors suggest that NK-CdM is an effective therapeutic candidate for preventing skin photoaging.

Acknowledgements

The authors would like to thank Green Cross LabCell Co., Ltd. for providing the conditioned medium of the natural killer cells.

Funding

The present study was supported by Green Cross WellBeing Corporation of Korea (grant no. 201809).

Availability of data and materials

The analyzed data sets generated during the study are available from the corresponding author on reasonable request.

Authors' contributions

SEL, TRK, CTO and BJK designed experiments. SEL, TRK, JHK and CTO performed the experiments. MI, BCL, YKH, SHP, SH, JYK and CTO analyzed data. YKH, SHP and SH prepared the materials. SEL and TRK prepared the figures. TRK wrote the manuscript. BJK and TRK edited the manuscript for final content. All authors have read and approved the final manuscript.

Ethics approval and consent to participate

All study samples were obtained after the acquisition of written informed consent from the study participants, in accordance with the Declaration of Helsinki. The research protocol was reviewed and approved by the Institutional Review Board of Seoul National University Hospital (permit no. H-1811-023-985).

Patient consent for publication

Not applicable.

Competing interests

The authors declare that they have no competing interests.

References

1. Makrantonaki E, Vogel M, Scharffetter-Kochanek K and Zouboulis CC: Skin aging: Molecular understanding of extrinsic and intrinsic processes. Hautarzt 66: 730-737, 2015 (Article in German).
2. Gonzaga ER: Role of UV light in photodamage, skin aging, and skin cancer: Importance of photoprotection. Am J Clin Dermatol 10 (Suppl 1): S19-S24, 2009.
3. Wenk J, Brenneisen P, Meewes C, Wlaschek M, Peters T, Blaudschun R, Ma W, Kuhr L, Schneider L and Scharffetter-Kochanek K: UV-induced oxidative stress and photoaging. Curr Probl Dermatol 29: 83-94, 2001.
4. Berneburg M, Plettenberg H and Krutmann J: Photoaging of human skin. Photodermatol Photoimmunol Photomed 16: 239-244, 2000.
5. Fisher GJ: The pathophysiology of photoaging of the skin. Cutis 75 (2 Suppl): S8-S9, 2005.
6. Scharffetter-Kochanek K, Brenneisen P, Wenk J, Herrmann G, Ma W, Kuhr L, Meewes C and Wlaschek M: Photoaging of the skin from phenotype to mechanisms. Exp Gerontol 35: 307-316, 2000.
7. Nishigori C: Cellular aspects of photocarcinogenesis. Photochem Photobiol Sci 5: 208-214, 2006.
8. Brenneisen P, Sies H and Scharffetter-Kochanek K: Ultraviolet-B irradiation and matrix metalloproteinases: From induction via signaling to initial events. Ann N Y Acad Sci 973: 31-43, 2002.
9. Vermeer BJ and Gilchrest BA: Cosmeceuticals. A proposal for rational definition, evaluation, and regulation. Arch Dermatol 132: 337-340, 1996.
10. Geesin JC, Darr D, Kaufman R, Murad S and Pinnell SR: Ascorbic acid specifically increases type I and type III procollagen messenger RNA levels in human skin fibroblast. J Invest Dermatol 90: 420-424, 1988.
11. Conti M, Couturier M, Lemonnier F and Lemonnier A: Antioxidant properties of vitamin E and membrane permeability in human fibroblast cultures. Adv Exp Med Biol 264: 125-128, 1990.
12. Cho HS, Lee MH, Lee JW, No KO, Park SK, Lee HS, Kang S, Cho WG, Park HJ, Oh KW and Hong JT: Anti-wrinkling effects of the mixture of vitamin C, vitamin E, pycnogenol and evening primrose oil, and molecular mechanisms on hairless mouse skin caused by chronic ultraviolet B irradiation. Photodermatol Photoimmunol Photomed 23: 155-162, 2007.
13. Hernández-Camacho JD, Bernier M, López-Lluch G and Navas P: Coenzyme Q10 supplementation in aging and disease. Front Physiol 9: 44, 2018.
14. Cos P, Rajan P, Vedernikova I, Calomme M, Pieters L, Vlietinck AJ, Augustyns K, Haemers A and Vanden Berghe D: In vitro antioxidant profile of phenolic acid derivatives. Free Radic Res 36: 711-716, 2002.
15. Kwon TR, Oh CT, Choi EJ, Kim SR, Jang YJ, Ko EJ, Yoo KH and Kim BJ: Conditioned medium from human bone marrow-derived mesenchymal stem cells promotes skin moisturization and effacement of wrinkles in UVB-irradiated SKH-1 hairless mice. Photodermatol Photoimmunol Photomed 32: 120-128, 2016.
16. Jayaraman P, Nathan P, Vasanthan P, Musa S and Govindasamy V: Stem cells conditioned medium: A new approach to skin wound healing management. Cell Biol Int 37: 1122-1128, 2013.
17. Sundaram H, Mehta RC, Norine JA, Kircik L, Cook-Bolden FE, Atkin DH, Werschler PW and Fitzpatrick RE: Topically applied physiologically balanced growth factors: A new paradigm of skin rejuvenation. J Drugs Dermatol 8 (5 Suppl Skin Rejuenation): S4-S13, 2009.
18. Lotzová E: Definition and functions of natural killer cells. Nat Immun 12: 169-176, 1993.
19. Vivier E, Tomasello E, Baratin M, Walzer T and Ugolini S: Functions of natural killer cells. Nat Immunol 9: 503-510, 2008.
20. Robertson MJ and Ritz J: Biology and clinical relevance of human natural killer cells. Blood 76: 2421-2438, 1990.
21. Lim O, Lee Y, Chung H, Her JH, Kang SM, Jung MY, Min B, Shin H, Kim TM, Heo DS, *et al*: GMP-compliant, large-scale expanded allogeneic natural killer cells have potent cytolytic activity against cancer cells in vitro and in vivo. PLoS One 8: e53611, 2013.
22. Min B, Choi H, Her JH, Jung MY, Kim HJ, Jung MY, Lee EK, Cho SY, Hwang YK and Shin EC: Optimization of large-scale expansion and cryopreservation of human natural killer cells for anti-tumor therapy. Immune Netw 18: e31, 2018.
23. Livak KJ and Schmittgen TD: Analysis of relative gene expression data using real-time quantitative PCR and the 2(-Delta Delta C(T)) method. Methods 25: 402-408, 2001.
24. Park BS, Jang KA, Sung JH, Park JS, Kwon YH, Kim KJ and Kim WS: Adipose-derived stem cells and their secretory factors as a promising therapy for skin aging. Dermatol Surg 34: 1323-1326, 2008.
25. Beanes SR, Dang C, Soo C and Ting K: Skin repair and scar formation: The central role of TGF-beta. Expert Rev Mol Med 5: 1-22, 2003.
26. Barrientos S, Stojadinovic O, Golinko MS, Brem H and Tomic-Canic M: Growth factors and cytokines in wound healing. Wound Repair Regen 16: 585-601, 2008.
27. Kim MS, Song HJ, Lee SH and Lee CK: Comparative study of various growth factors and cytokines on type I collagen and hyaluronan production in human dermal fibroblasts. J Cosmet Dermatol 13: 44-51, 2014.
28. Werb Z: ECM and cell surface proteolysis: Regulating cellular ecology. Cell 91: 439-442, 1997.
29. Lukashev ME and Werb Z: ECM signalling: Orchestrating cell behaviour and misbehaviour. Trends Cell Biol 8: 437-441, 1998.
30. Pillai S, Oresajo C and Hayward J: Ultraviolet radiation and skin aging: Roles of reactive oxygen species, inflammation and protease activation, and strategies for prevention of inflammation-induced matrix degradation-a review. Int J Cosmet Sci 27: 17-34, 2005.
31. Kammeyer A and Luiten RM: Oxidation events and skin aging. Ageing Res Rev 21: 16-29, 2015.
32. Rittié L and Fisher GJ: UV-light-induced signal cascades and skin aging. Ageing Res Rev 1: 705-720, 2002.
33. Muthusamy V and Piva TJ: The UV response of the skin: A review of the MAPK, NFkappaB and TNFalpha signal transduction pathways. Arch Dermatol Res 302: 5-17, 2010.
34. Brohem CA, Cardeal LB, Tiago M, Soengas MS, Barros SB and Maria-Engler SS: Artificial skin in perspective: Concepts and applications. Pigment Cell Melanoma Res 24: 35-50, 2011.